AJNR

MR Imaging of Pineal Tumors

Robert D. Tien, A. J. Barkovich and M. S. B. Edwards

AJNR Am J Neuroradiol 1990, 11 (3) 557-565
http://www.ajnr.org/content/11/3/557

MR Imaging of Pineal Tumors

Robert D. Tien[1]
A. J. Barkovich[1,2]
M. S. B. Edwards[2]

MR images of pineal region tumors were analyzed in 26 patients with histologically proved tumors: seven germ-cell tumors, six astrocytomas, five teratomas, three pineoblastomas, two meningiomas, one dermoid, one epidermoid, and one metastasis. In an attempt to identify specific MR characteristics of these lesions, Gd-DTPA was administered to six patients. CSF and blood serum were assayed for alpha-fetoprotein (AFP) and human chorionic gonadotropin–beta subunit (HCG-β) in 18 patients. MR findings were correlated with age, sex, the presence of biochemical tumor markers, and surgical outcome. We found that the most important factors in the determination of tumor type were the patient's age and the tumor markers. Increased levels of both HCG-β and AFP were specific for patients with malignant teratomas and undifferentiated germ-cell tumors. HCG-β alone was elevated in the patient with choriocarcinoma; only AFP was elevated in the patient with an endodermal sinus tumor. Tumor markers were not present in other patients in this series. The tumor size and the presence of fat were also helpful in determining tumor type. Hemorrhage was rare, seen only in the patient with a choriocarcinoma. Gd-DTPA did not enhance diagnostic specificity but aided in the detection of tumor seeding through CSF.

We conclude that, although MR is sensitive in the detection of pineal region tumors and provides superb anatomic detail, MR signal characteristics are usually nonspecific. Correlation with the patient's age and the tumor markers significantly improves diagnostic accuracy.

***AJNR* 11:557–565, May/June 1990; *AJR* 155: July 1990**

Pineal region tumors constitute 3–8% of intracranial tumors in children [1] and 0.4–1.0% of brain tumors in adults [2]. Although germinomas and astrocytomas account for the majority of tumors in this area, at least 17 histologically distinct tumor types may occur in the pineal region [3]. Advances in diagnostic and surgical techniques have significantly improved surgical outcome in these patients; nonetheless, complete surgical resection of tumors in this region is extremely difficult. Chemotherapy and radiation remain the major therapeutic methods. It has been reported recently, however, that 36–50% of pineal tumors are either benign or radioresistant [1, 4]. Because the different pineal tumors require different combinations of chemotherapeutic agents and radiation for optimal therapy, accurate assessment of tumor histology and accurate means of following tumor response are essential for optimal therapy. We retrospectively reviewed the MR studies of 26 patients with histologically proved pineal region tumors treated between 1984 and 1988 at the University of California, San Francisco. Eighteen of them had assays of blood serum and CSF for human chorionic gonadotropin–beta subunit (HCG-β) and alpha-fetoprotein (AFP); the results of these assays are correlated with imaging and histologic findings.

Materials and Methods

MR imaging studies of 26 patients (22 males and four females) with histologically proved pineal region tumors were reviewed retrospectively. The patients were 3 months to 70 years

Received July 10, 1989; revision requested August 29, 1989; final revision received November 9, 1989; accepted November 14, 1989.

[1] Department of Radiology, Neuroradiology Section, University of California, San Francisco, CA 94143-0628. Address reprint requests to A. J. Barkovich.

[2] Department of Neurological Surgery, Division of Pediatric Neurosurgery, University of California, San Francisco, CA 94143-0112.

0195–6108/90/1103–0557

TABLE 1: Serum Tumor Markers Assayed in 18 Patients with Pineal Tumors

Type of Tumor	No. Assayed	Elevated AFP	Elevated HCG-β	Both Elevated	Neither Elevated
Germinoma	4	0	0	0	4
Malignant teratoma	4	0	0	2	2
Endodermal sinus tumor	1	1	0	0	0
Choriocarcinoma	1	0	1	0	0
Undifferentiated germ-cell tumor	1	0	0	1	0
Astrocytoma	4	0	0	0	4
Teratoma	1	0	0	0	1
Pineoblastoma	2	0	0	0	2
Total	18	1	1	3	13

Note.—AFP = alpha-fetoprotein; HCG-β = human chorionic gonadotropin–beta subunit.

TABLE 2: Summary of Patients with Pineal Tumors

Tumor Type/ Case No.	Age (years)	Sex	Symptoms	Size (cm)/ Shape	Sites of Invasion	Fat or Blood	MR Characteristics		Hydrocephalus	Spread in CSF
							T1	T2		
Germinoma										
1[a]	19	M	PS, DI	2.5 × 1.5 × 2.5/ lobulated	Pineal region, tectum	No	Isointense relative to GM; small cystic necrotic area	Slightly hyperintense relative to GM	–	Yes[b,c]
2[a]	10	M	PS, DI	1.5 × 1.5 × 1.5	Pineal region, tectum, tegmentum	No	Isointense	Slightly hyperintense relative to GM	–	Yes[b]
3	17	F	Headache, impotence	2 × 2 × 2/round	Tectum, tegmentum, thalamus, midbrain	No	Isointense	Slightly hyperintense relative to GM	–	No
4[a]	20	M	PS, DI	1.5 × 1.5 × 1.5/ lobulated	Tectum, posterior commissure	No	Isointense with multiple small cysts	Slightly hyperintense relative to GM	+	Yes[b]
Astrocytoma										
5	8	M	Headache, diplopia	2 × 2 × 2/round	Tectum, tegmentum	No	Isointense	Hyperintense	–	No
6	8	M	Headache, diplopia	2.7 × 2.7 × 2/ round	Tectum, tegmentum, thalamus	No	Isointense with small low-signal cysts	Hyperintense	–	No
7	18	M	Headache, nausea	2 × 2 × 2/ovoid	Tectum, tegmentum	No	Isointense	Hyperintense	+	No
8	35	F	Headache	2 × 2 × 2/ovoid	Tectum	No	Hypointense, cystic	Hyperintense	+	No
9	36	M	Headache	1.5 × 1.5 × 2/ round	Chorioid fissure, tectum, superior vermis	No	Hypointense	Hyperintense	–	No
10[a]	14	M	Headache	3 × 3 × 2.5/ round	Tectum	No	Isointense	Hyperintense	+	No
Pineoblastoma										
11	0	M	Increased head girth	4.3 × 3 × 2/lobulated	Tectum	No	Isointense, small cystic necrotic area	Iso- to slightly hyperintense	+	No
12	4	M	Headache, visual disturbance	2 × 3 × 2/lobulated	Tectum, vermis	No	Isointense	Iso- to slightly hyperintense	+	No
13[a]	66	F	Headache, nausea, vomiting	4 × 4 × 4/lobulated	Tectum, thalamus, R corpus callosum, tegmentum	No	Hypointense	Iso- to slightly hyperintense	+	No
Undifferentiated germ-cell tumor										
14	9	M	Headache	2 × 2 × 3/ovoid	Tectum, bilateral tegmentum, thalamus	No	Isointense	Hyperintense	+	No

TABLE 2—*Continued*

Tumor Type/ Case No.	Age (years)	Sex	Symptoms	Size (cm)/ Shape	Sites of Invasion	Fat or Blood	MR Characteristics		Hydrocephalus	Spread in CSF
							T1	T2		
Endodermal sinus tumor										
15	16	M	Headache	2 × 2 × 2/round	Midbrain, thalamus	No	Isointense	Inhomogeneous, hyperintense	+	No
Choriocarcinoma										
16	16	M	Intermittent headache	2.5 × 2.5 × 3/ovoid	Tectum, tegmentum, corpus callosum	Yes (blood)	Hyperintense	Hyperintense	+	No
Dermoid										
17	18	M	Headache	3 × 4 × 4/ovoid	No invasion	Yes (fat)	Hyperintense with calcifications	Isointense	–	No
Epidermoid										
18	52	M	Personality change	3 × 3 × 2.5/lobulated	Irregular displacement	No	Hypointense	Hyperintense	–	No
Meningioma										
19	70	F	Headache	2 × 2 × 2.5/round	Displaced corpus callosum	No	Isointense; calcifications	Hyperintense	+	No
20	50	M	Asymptomatic	2 × 2 × 3.5/round	Displaced corpus callosum	No	Isointense	Isointense	+	No
Metastasis, oat-cell carcinoma of lung										
21	68	M	Metastasis workup	1.5 × 2.5 × 1.5/ovoid	Tectum	No	Hypointense	Isointense	+	No
Teratoma										
22	17	M	Headache	4 × 3 × 2.5/ovoid	No invasion	Yes (fat)	Mixed high & low signal	Hyperintense with low signal	+	No
Malignant teratoma										
23	7	M	Headache, diplopia papilledema	6 × 6 × 6.5/ovoid	Tectum, cerebellar hemisphere, midbrain, thalamus	No	Slightly hypointense	Heterogeneous, hyperintense	+	No
24	8	M	Headache	2 × 2 × 2/irregular cyst	Tectum, tegmentum	No	Inhomogeneous, hypointense	Inhomogeneous hyperintense	+	No
25[a]	15	M	Headache, PS	5 × 3 × 2/irregular	Tectum, floor of third ventricle	No	Slightly hypointense	Hyperintense	+	Yes[d]
26	18	M	Headache, nausea	3 × 4 × 2.5/irregular	Tectum, bilateral tegmentum, thalamus, L choroid fissure, L temporal horn	No	Slightly hypointense	Hyperintense	+	No

Note.—PS = Parinaud syndrome; DI = diabetes insipidus; GM = gray matter; R = right; L = left.

[a] Gd-DTPA was administered in this patient.

[b] Thickened pituitary stalk with absence of high signal intensity of posterior pituitary lobe on T1-weighted images, compatible with subependymal metastasis to hypothalamus and pituitary.

[c] Subependymal metastasis with bright signal at left frontal horn and right trigone, which enhanced with Gd-DTPA.

[d] CSF metastases noted in spinal canal by Gd-DTPA–enhanced MR.

old (mean, 23.5 years). At presentation, most patients (19/26) had headaches, seven patients had abnormal eye movements (including four patients with Parinaud syndrome), and three patients had diabetes insipidus.

Most of the MR images (23/26) were obtained on a 1.5-T superconductive imager (Signa, General Electric, Milwaukee, WI) using standard protocols. Sagittal spin-echo (SE) images were obtained by using a sequence of 600/20/2 (TR/TE/excitations). Axial images were obtained by using an SE 2500–2800/30–80 sequence. Additional SE 600/20 images were obtained after infusion of Gd-DTPA in six patients. Three patients were studied with a 0.35-T Diasonics MT/S scanner; sagittal SE 500/30 and axial SE 2000/40–80 images were obtained. All images were acquired with the use of a standard head coil, 256 × 256 matrix, 20-cm field of view, and 3- to 5-mm slice thickness. A 1-mm gap was used on short TR sequences and a 2.5-mm interslice gap was used on long TR sequences.

The size, shape, location, local invasion (lack of clear-cut tissue planes between tumor and adjacent structures), and signal charac-

teristics of each tumor were carefully correlated with patient's demographic information and histopathologic results. Signal intensities of tumors were compared with those of the hemispheric white or gray matter on short TR/short TE and long TR/long TE pulse sequences. The CSF and blood serum tumor markers (AFP [normal, <5 ng/ml] and HCG-β [normal, <2 ng/ml]) were assayed in 18 patients and the results were correlated with the histopathologic diagnosis in these patients.

Results

Tumor Markers (Table 1)

The patient with choriocarcinoma had extremely elevated (2300 ng/ml) HCG-β levels in serum and CSF but normal AFP levels. Both HCG-β and AFP levels were elevated in two of four patients with malignant teratomas and in the patient with an undifferentiated germ-cell tumor. Tissue from the other two patients with malignant teratoma stained positive for both HCG-β and AFP but neither CSF nor serum levels were elevated. AFP levels were elevated but HCG-β levels were normal in the patient with an endodermal sinus tumor. All tumor markers were normal in germinomas, astrocytomas, pineoblastomas, the benign teratoma, the dermoid, and epidermoid tumors in this series.

MR Characteristics (Table 2)

Hydrocephalus was present in 18 patients; it was conspicuously absent in three of the four germinomas, three of the six astrocytomas, and the single epidermoid and dermoid tumors. Hydrocephalus was diagnosed by the presence of enlarged ventricles or ventriculostomy tubes.

Germinomas.—This group comprised four adolescent males (average age, 17 years old). All masses were isointense relative to normal white matter on T1-weighted images and slightly hyperintense relative to white matter on T2-weighted images. In two of the four patients, some small cystic areas were noted (Fig. 1A); in the other two, the masses were homogeneous. All the masses invaded the tectum. Three patients had evidence of CSF spread to the infundibular recess of the third ventricle; all three had diabetes insipidus and Parinaud syndrome at initial presentation. Hydrocephalus was present in one of these three patients. Gd-DTPA was given to one patient; the pineal mass enhanced intensely and heterogeneously (Fig. 1B). Furthermore, enhancing subependymal metastases were seen in the hypothalamus, left frontal horn, and right trigone (Fig. 1C).

Benign teratoma.—One patient, a 17-year-old male boy, had an ovoid mass with areas of heterogeneous high and low signal intensity on T1-weighted images (Fig. 2A). On T2-weighted images the mass showed heterogeneous high signal intensity. Foci of calcification noted on CT (Figs. 2B and 2C) were represented by low signal on both T1– and T2-weighted images. There was no evidence of local invasion.

Malignant teratoma.—These tumors were found in four boys (average age, 12 years). Two of the four masses were large (greater than 5 cm in at least one dimension). The other two masses were smaller but irregular in shape. They were all heterogeneous and hypointense relative to brain with areas of low signal intensity on T1-weighted images and areas of high signal intensity on T2-weighted images (Fig. 3). This heterogeneous component represented a mixture of foci of calcification and/or cystic-necrotic areas detected by prior CT studies. These tumors all invaded the tectum and tegmentum (Fig. 3A). The largest one invaded the cerebellum, thalamus, midbrain, and cerebral hemisphere (Fig. 3). The second largest one filled the entire third ventricle and had CSF metastases to the lumbar spinal canal.

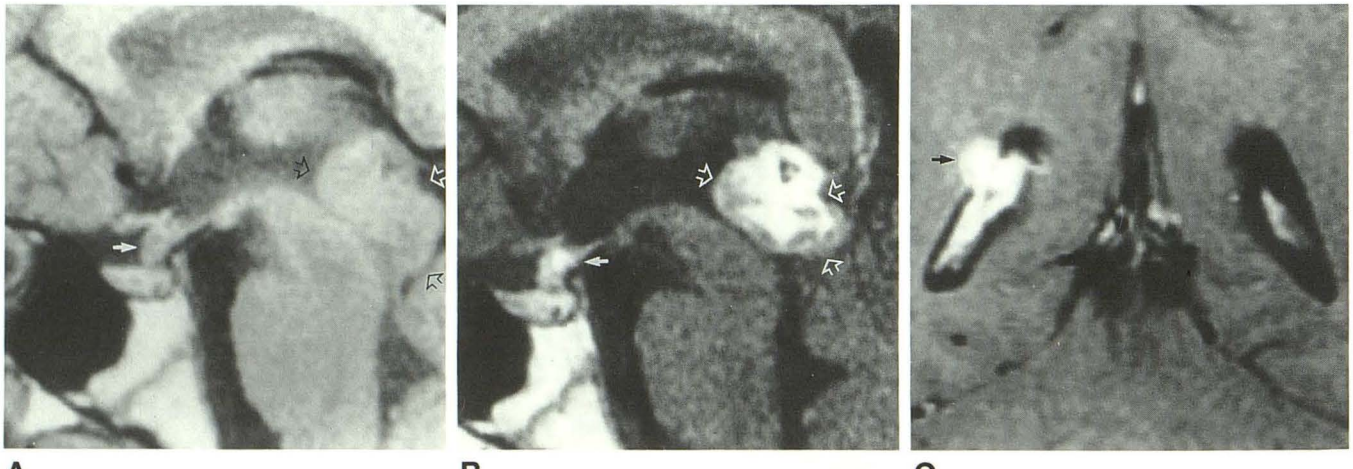

Fig. 1.—Case 1: Hypothalamic metastasis from pineal germinoma.

***A*, Sagittal SE 600/20 image reveals 2.5 × 1.5 × 2.5 cm lobulated mass in pineal region (*open arrows*) that is isointense relative to gray matter, with small cystic necrotic areas. Pituitary infundibulum is thickened (*solid arrow*) and high signal intensity of posterior pituitary is absent, consistent with history of diabetes insipidus.**

***B*, Sagittal SE 600/20 image after infusion of Gd-DTPA shows heterogeneous enhancement of pineal mass (*open arrows*) and enhancing nodule in median eminence (*solid arrow*).**

***C*, Coronal SE 600/20 image after infusion of Gd-DTPA reveals enhancing subependymal metastatic nodule (*arrow*) at right trigone.**

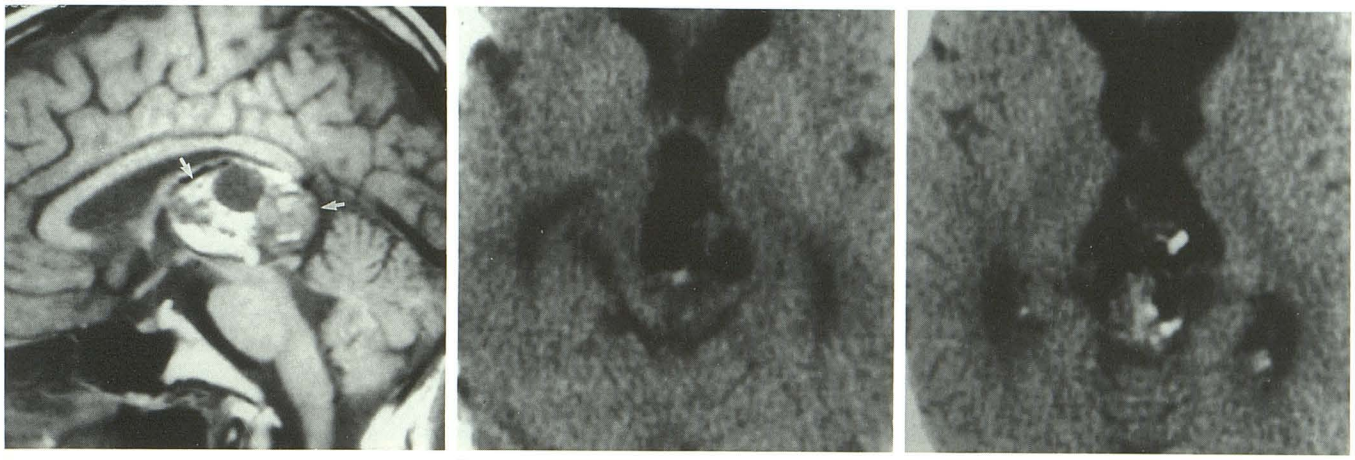

Fig. 2.—Case 22: Benign teratoma.
A, Sagittal SE 600/20 image shows oval mass in pineal region and third ventricle (*arrows*) with heterogeneous areas of high and low signal intensity within it.
B and *C*, Unenhanced CT scans show calcification and fatty components within mass.

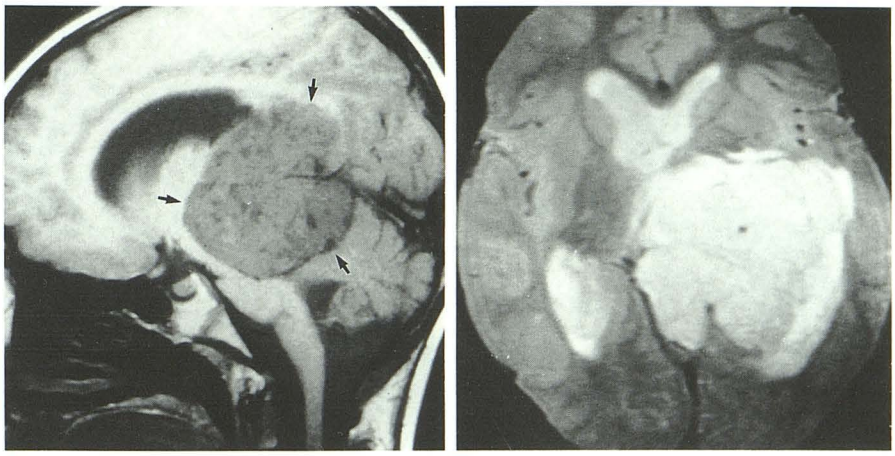

Fig. 3.—Case 23: Malignant teratoma.
A, Sagittal SE 600/20 image shows large lobulated pineal mass (*arrows*), which is hypointense relative to gray matter with some foci of low signal intensity. Tumor invades tectum, tegmentum, cerebellum, and corpus callosum.
B, Axial SE 2800/80 image shows slightly heterogeneous, hyperintense mass invading left lateral ventricle and thalamus.

Endodermal sinus tumor.—One patient, a 16-year-old boy, had a round mass that was isointense relative to white matter on T1-weighted images. On T2-weighted images, a heterogeneous high signal intensity was noted. The tumor invaded the midbrain and thalamus.

Choriocarcinoma.—One patient, a 16-year-old boy, had an infiltrating mass that was heterogeneous with a large hemorrhagic component on T1- and T2-weighted images; angiography showed neovascularity with multiple small areas of aneurysmal dilatation (Fig. 4). The mass invaded the tectum, tegmentum, splenium of the corpus callosum, and lateral ventricle.

Undifferentiated germ-cell tumor.—One patient, a 9-year-old boy, had an ovoid mass that was isointense relative to gray matter on T1-weighted images and hyperintense on T2-weighted images. Invasion of the tectum and tegmentum was noted.

Astrocytomas.—This group comprised five males (average age, 17 years old) and one 35-year-old woman. One of the six astrocytomas was cystic, invaded the mesencephalic tectum, and caused hydrocephalus (Fig. 5). The mass was hypointense relative to gray matter on T1-weighted images and hyperintense on T2-weighted images. The other five masses were round or ovoid, either iso- or hypointense relative to gray matter on T1-weighted images, and hyperintense on T2-weighted images (Fig. 6). They all invaded the tectum and/or tegmentum.

Pineoblastomas.—The patients with pineoblastomas included two boys (6 months and 4 years old) and one 66-year-old woman. Two of these masses were large, with one dimension 4 cm or greater. These lobulated masses all had several cystic-necrotic areas. The solid portions of the tumors were nearly isointense relative to gray matter on T1- and T2-weighted images. They invaded thalamus (1/3), tectum (3/3),

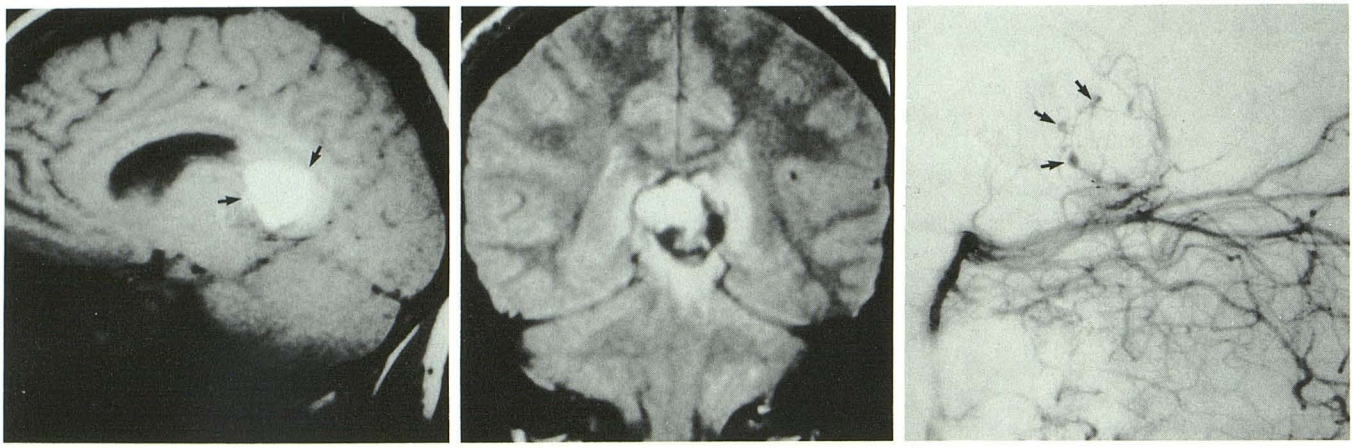

Fig. 4.—Case 16: Choriocarcinoma.
A, Sagittal SE 600/20 image shows hyperintense pineal region mass (*arrows*) infiltrating splenium of corpus callosum and lateral ventricle.
B, Coronal SE 2800/80 image shows heterogeneous high- and very-low-signal mass with infiltration into tectum and tegmentum. High and low signal was due to hemorrhagic component found at surgery.
C, Lateral projection of vertebral arteriogram shows multiple small areas of aneurysmal dilatation in this mass (*arrows*). Arterial supply was mainly from posterior choroidal arteries.

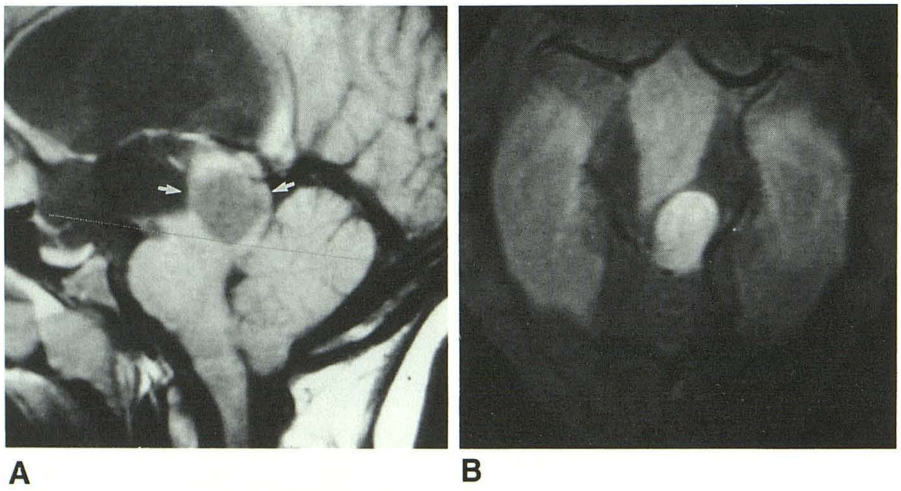

Fig. 5.—Case 8: Astrocytoma (moderately anaplastic).
A, Sagittal SE 600/20 image shows ovoid pineal region mass involving tectum (*arrows*) with hypointense central component. Aqueduct is compressed and marked obstructive hydrocephalus is present.
B, Axial SE 2000/80 image. Mass is hyperintense relative to gray matter and CSF. Central component was found to be cystic at surgery.

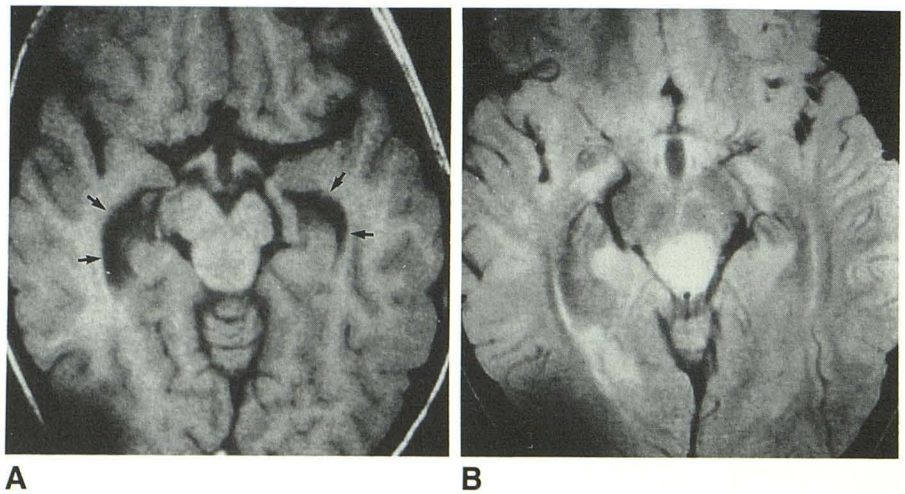

Fig. 6.—Case 7: Astrocytoma (moderately anaplastic).
A, Axial SE 600/20 image shows isointense, bulbous mass involving tectum and obliterating aqueduct. Mild dilatation of temporal horns from obstructive hydrocephalus is seen (*arrows*).
B, Axial SE 2800/80 image better defines mass, which has prolonged T2 relaxation.

tegmentum (1/3), corpus callosum (1/3), and cerebellar vermis (1/3). The female patient received Gd-DTPA, resulting in homogeneous tumor enhancement (Fig. 7).

Meningiomas.—These two patients (a 70-year-old woman and a 50-year-old man) had round masses that were isointense relative to gray matter on T1-weighted images and iso- to slightly hyperintense relative to gray matter on T2-weighted images. One of the two masses had an area of calcification, detected by CT, which was of low signal intensity on both T1- and T2-weighted images. The masses smoothly displaced the splenium of the corpus callosum without evidence of invasion (Fig. 8).

Metastasis.—The mass in this one patient, a 68-year old man with oat cell carcinoma of the lung, was hypointense relative to gray matter on T1-weighted images, was isointense relative to gray matter on T2-weighted images, and invaded the tectum.

Dermoid.—This large ovoid pineal region mass was present in one patient. It was hyperintense relative to gray matter on T1-weighted images and isointense on T2-weighted images, consistent with the lipid character of the lesion (Fig. 9). There was displacement of the corpus callosum and tectum, but no evidence of invasion.

Epidermoid.—The lobulated mass found in one patient was of very low signal intensity on T1-weighted images and was hyperintense relative to gray matter (generally isointense relative to CSF) on T2-weighted images with some heterogeneity on both. Irregular displacement of surrounding structures was noted (Fig. 10).

Discussion

Pineal region tumors constitute 3–8% of intracranial tumors in children [1] and 0.4–1% of brain tumors in adults [2]. When these tumors occlude the cerebral aqueduct, obstructive hydrocephalus with intracranial hypertension results. If the superior colliculus and pretectal areas are involved, characteristic ophthalmologic signs develop: impairment of upward

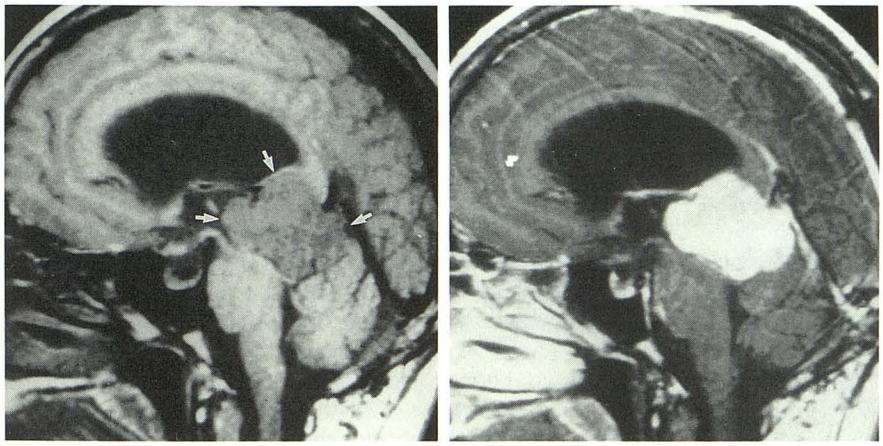

Fig. 7.—Case 13: Pineoblastoma.
A, Sagittal SE 600/20 image shows large, slightly hypointense mass (*arrows*) in pineal region, infiltrating splenium of corpus callosum, tectum, tegmentum, and superior vermis. Note irregular, poorly defined splenium-tumor junction. Low-intensity, necrotic foci were seen on parasagittal images. At surgery, invasion of splenium was found.
B, Sagittal SE 600/20 image after infusion of Gd-DTPA shows homogeneous enhancement of mass.

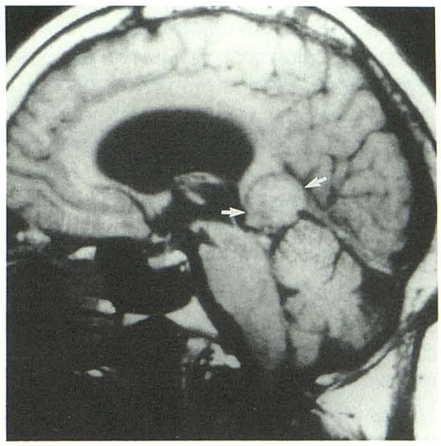

Fig. 8.—Case 20: Meningioma. Sagittal SE 600/20 image shows round, isointense mass (*arrows*) in pineal region, displacing but not invading splenium of corpus callosum and tectum. Tissue planes are well preserved (compare with Fig. 7). Mild obstructive hydrocephalus is noted.

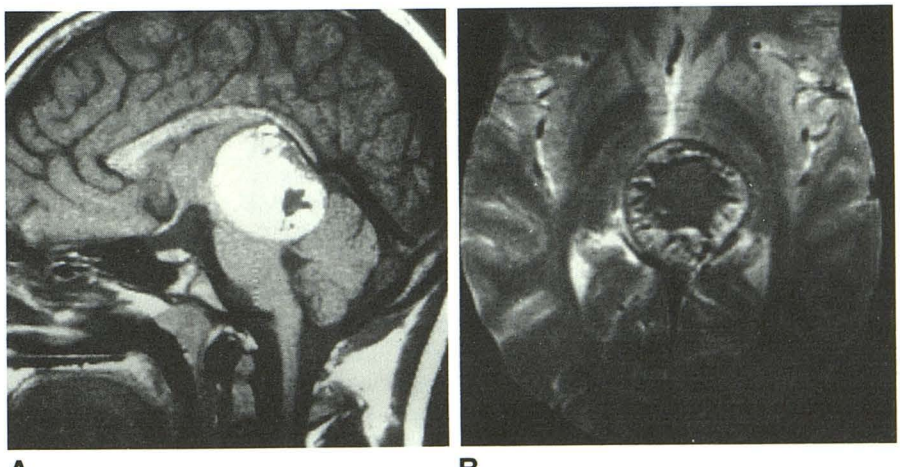

Fig. 9.—Case 17: Dermoid.
A, Sagittal SE 600/20 image reveals large pineal mass that is hyperintense relative to brain with foci of very low signal; corpus callosum is displaced but not invaded. Foci of low signal were proved at surgery to be calcification.
B, On axial T2-weighted SE 2800/80 image, mass is isointense relative to white matter. Short T2 is consistent with lipid and is characteristic of dermoids.

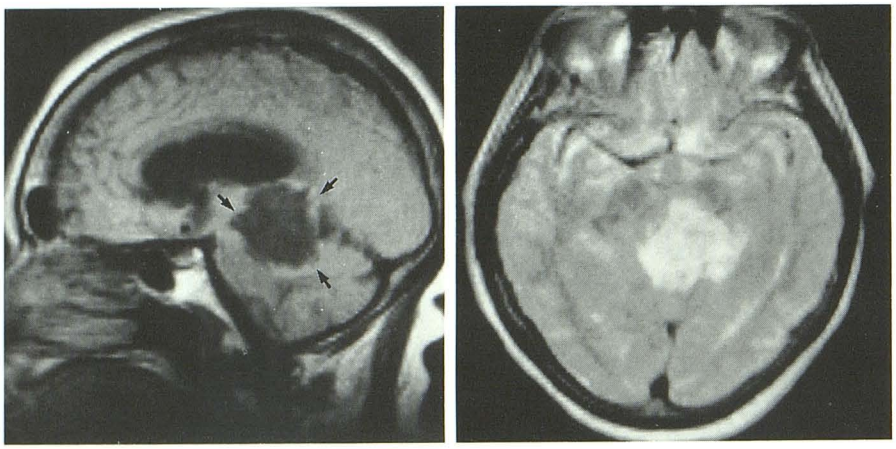

Fig. 10.—Case 18: Epidermoid.
A, Sagittal SE 600/20 image shows lobulated, hypointense mass (*arrows*) in pineal region, which has slight internal heterogeneity. Aqueduct was not identified, but there was no evidence of hydrocephalus.
B, Axial SE 2000/80 shows mass is generally isointense relative to CSF with heterogeneity.

gaze, abnormalities of the pupil, paralysis or spasm of convergence, and nystagmus retractorius; this is the so-called sylvian aqueduct syndrome. Parinaud syndrome, the paralysis of upward gaze, is caused by compression or invasion of the mesencephalon just ventral to the aqueduct and caudal to the posterior part of the third ventricle. When there is suprasellar involvement, diabetes insipidus is a common presentation; less common symptoms include precocious puberty or delayed onset of sexual maturation.

Because pineal region tumors are among the most dangerous intracranial masses to excise completely, early attempts at surgery in this location produced high mortality and morbidity rates; the early literature therefore reflects a strong bias for treatment that is limited to ventricular shunting followed by radiation therapy [4–8]. However, at least 17 histologically distinct tumor types may occur in the pineal region [3], approximately 10% of which are benign (including cysts, lipomas, pineal cysts, and meningiomas). Another 5–10% are relatively benign and not responsive to radiation. In fact, it has been reported recently that 36–50% of pineal tumors are either benign or are radioresistant [1, 4]. Furthermore, as a result of advances in microsurgical techniques, the mortality and morbidity rates associated with pineal region surgery have diminished significantly. Biopsy before the initiation of therapy has therefore been recommended in the more recent surgical literature [1, 3, 9].

The optimal therapy for different pineal tumors is different combinations of surgery, chemotherapy, and radiotherapy, the exact combination being dependent on tumor histology. However, tumors with complex and mixed histologic patterns, which are common in the pineal region, make diagnosis by needle biopsy inaccurate. Moreover, the complex nature of the tumors in this region makes the imaging characteristics nonspecific, as has been evident from the CT literature [10, 11].

MR has provided a marked improvement in the localization and characterization of tumors as a result of facile multiplanar imaging and superior tissue contrast and resolution [12, 13]. In a few instances in our series, the correct histologic diagnosis could be deduced on the basis of MR findings, such as tumor size and signal characteristics, and clinical findings, such as patient age, sex, and presenting symptoms. Gd-DTPA administration facilitated the detection of the subependymal or "drop" spinal metastasis in malignant pineal tumors, making the staging of the tumor much more accurate but did not aid in diagnostic specificity.

The following observations are of some importance in the MR diagnosis of pineal region tumors. Pineoblastomas and malignant teratomas tended to be large (>4 cm) and irregular in shape, differentiating them from most other tumors, which were round or ovoid and about 2–3 cm in diameter at presentation. Only the dermoid and benign teratoma had a characteristic fat signal; surprisingly, fat was not seen in any of the malignant teratomas. That hemorrhage was recognized only in the single choriocarcinoma was not surprising in view of their propensity to bleed; the presence of hemorrhage seems rather specific and should suggest choriocarcinoma. Round, well-defined, homogeneous tumors displacing the surrounding structures without invasion in an older individual will most likely be meningiomas, whereas tumors clearly originating from the mesencephalon or surrounding temporal lobes are most likely gliomas. Young boys with diabetic insipidus and Parinaud syndrome usually have a pineal region tumor with subependymal metastasis to the hypothalamus; statistically, these are most likely germinomas. Overall, however, because of the tendency of most of these neoplasms to invade surrounding structures and because of the frequently mixed histology of the germ-cell tumors, histologic diagnosis without biopsy is unreliable.

It should be noted that the MR detection and differentiation of hemorrhage, calcification, and fat are complex. Hyperintensity on short TR scans may be seen in association with any intensity on long TR scans in hemorrhage, depending on the stage of evaluation of the hemorrhage [14]. Thus, the presence of hyperintensity on short TR images and hypointensity on long TR images, which is typical of fat, may rarely be seen in hemorrhage, although some hyperintensity is usually present on the long TR images [14]. Moreover, dermoids may occasionally be bright on both short TR and long TR images, and high signal on short TR images may be produced by high protein concentration [15]. Furthermore, foci of low signal intensity on both SE and gradient-echo MR images may be the result of chronic hemorrhage as well as calcium. The use of fat-suppression techniques [16] may be

helpful in the differentiation of fat from blood; however, on occasion, CT may be useful as an adjunct to MR in making this differentiation.

Our understanding of the pathology of brain tumors has increased considerably in recent years as a result of the discovery of biochemical markers that can be demonstrated in serum, CSF, and neurosurgical tissue specimens by immunocytochemical techniques. HCG-β and AFP are specific, useful markers for pineal region tumors. Choriocarcinomas or germ-cell tumors with syncytiotrophoblastic giant cells can produce HCG-β and stimulate the testes to produce testosterone, resulting in pseudoprecocious puberty [17–19]. Elevated CSF or serum levels of AFP with normal HCG-β always suggest a malignant germ-cell tumor, most often endodermal sinus tumor [3, 20–22]. Elevation of both markers can be seen in embryonal cell carcinomas, malignant teratomas, or mixed germ-cell tumors [3, 22]. Both CSF and serum AFP and HCG-β levels can be used as indicators of the efficacy of various treatments and as a check on the recurrence of tumors [14, 21, 23–25].

Until recently, germinomas, the most common intracranial germ-cell tumors [26], had not been identified as having a specific biochemical tumor marker [14, 27, 28]. However, serum and CSF values of placental alkaline phosphatase have recently been suggested as specific tumor markers for germinomas, especially with the highly sensitive enzyme-linked immunosorbent assay method [29, 30]. Although there are no biologic tumor markers to diagnose pineal parenchymal tumors, assay for the pineal hormone melatonin (MLT), which is secreted in a circadian rhythm with high serum levels during the daytime, may be useful. Both parenchymal and nonparenchymal tumors may interfere with the regulatory mechanisms of producing MLT. Thus, before surgery, MLT deficiency rather than exaggerated serum levels may be used as a marker for nonspecific pineal tumors that destroy the pineal gland. After tumor resection, serum MLT may serve to demonstrate complete pinealectomy [14, 31]. Elevation of CSF polyamine (putrescine and spermidine) in malignant brain tumors of childhood, especially primitive neuroectodermal tumors, has been reported [32].

In conclusion, although MR is sensitive in the detection of pineal region tumors and provides superb anatomic detail, the tumor signal characteristics are usually nonspecific. Correlation with the patient's age and tumor markers significantly improves diagnostic accuracy. Imaging both before and after administration of IV paramagnetic contrast material in six of our cases improved tumor staging but did not appear to significantly improve diagnostic accuracy. A combination of MR, biopsy, and assay for tumor markers is necessary for optimal diagnosis and management.

REFERENCES

1. Hoffman HJ, Yoshida M, Becker LE, et al. Pineal region tumors in childhood. Experience at the Hospital for Sick Children. In: Humphreys RP, ed. *Concepts in pediatric neurosurgery 4.* Basel: Karger, **1983**:360–386
2. Russel DS, Rubinstein LJ. *Pathology of tumours of the nervous system.* 4th ed. Baltimore: Williams & Wilkins, **1977**:284–295
3. Edwards MS, Hudgins RJ, Wilson CB, Levin VA, Wara WM. Pineal region tumors in children. *J Neurosurg* **1988**;68:689–697
4. Demakas JJ, Sonntag VKH, Kaplan AM, et al. Surgical management of pineal area tumors in early childhood. *Surg Neurol* **1982**;17:435–440
5. Abay EO II, Laws ER Jr, Grado GL, et al. Pineal tumors in children and adolescents. Treatment by CSF shunting and radiotherapy. *J Neurosurg* **1981**;55:889–895
6. Allen JC, Nisselbaum J, Epstein F, et al. Alphafetoprotein and human chorionic gonadotropin determination in cerebrospinal fluid. An aid to the diagnosis and management of intracranial germ-cell tumors. *J Neurosurg* **1979**;51:368–374
7. Chapman PH, Linggood RM. The management of pineal area tumors: a recent reappraisal. *Cancer* **1980**;46:1253–1257
8. Poppen JL, Marino R Jr. Pinealomas and tumors of the posterior portion of the third ventricle. *J Neurosurg* **1968**;28:357–364
9. Rand RW, Lemmon LJ. Tumors of the posterior portion of the third ventricle. *J Neurosurg* **1953**;10:1–8
10. Ganti SR, Hilal SK, Stein BM, Silver AJ, Mawad M, Sane P. CT of pineal region tumors. *AJR* **1986**;146:451–458
11. Futrell NN, Osborn AG, Cheson BD. Pineal region tumors: computed tomographic–pathologic spectrum. *AJR* **1981**;137:951–956
12. Muller-Forell W, Schroth G, Egan PJ. MR imaging in tumors of the pineal region. *Neuroradiology* **1988**;30:224–231
13. Kilgore DP, Strother CM, Starshak RJ, Haughton VM. Pineal germinoma: MR imaging. *Radiology* **1986**;158:435–438
14. Gomori JM, Grossman RI, Goldberg HI, Zimmerman RA, Bilaniuk LT. Intracranial hematomas: imaging by high field MR. *Radiology* **1985**;157:87–93
15. Som PM, Dillon WP, Fullerton GD, Zimmerman RA, Rajagopalan B, Marom Z. Chronically obstructed sinonasal secretions: observations on T1 and T2 shortening. *Radiology* **1989**;172:515–520
16. Simon J, Szumonowski J, Totterman S, et al. Fat-suppression MR imaging of the orbit. *AJNR* **1988**;9:961–968
17. Fetell MR, Stein BM. Neuroendocrine aspects of pineal tumors. *Neurol Clin* **1986**;4:877–905
18. Bjornsson J, Scheithauer BW, Leech RW. Primary intracranial choriocarcinoma: a case report. *Clin Neuropathol* **1986**;5:242–245
19. Grasiano SL, Paolozzi FP, Rudolph AR, Steward WA, Elbadawi A, Comis RL. Mixed germ-cell tumor of the pineal region: case report. *J Neurosurg* **1987**;66:300–304
20. Talerman A. Germ cell tumors. *Ann Pathol* **1985**;5:145–157
21. Kida Y, Kobayashi T, Yoshida J, Kato K, Kageyama N. Chemotherapy with cisplatin for AFP-secreting germ-cell tumors of the central nervous system. *J Neurosurg* **1986**;65:470–475
22. Howlett TA, Senoussi M, Fox JL, Woodhouse NJ. Puberty due to a mixed germ-cell tumour of the hypothalamus secreting β-HCG and alpha-fetoprotein. *Horm Res* **1987**;25:13–17
23. Allen JC, Nisselbaum J, Epstein E, et al. Alpha fetoprotein and human chorionic gonadotropin determination in cerebrospinal fluid. An aid to the diagnosis and management of intracranial germ-cell tumors. *J Neurosurg* **1979**;51:368–374
24. Arita N, Ushio Y, Hayakawa T, et al. Serum levels of alpha-fetoprotein, human chorionic gonadotropin and carcinoembryonic antigen in patients with primary intracranial germ cell tumors. *Oncodev Biol Med* **1980**;1:235–240
25. Jennings MT, Gelman R, Hochberg F. Intracranial germ-cell tumors: natural history and pathogenesis. *J Neurosurg* **1985**;63:155–167
26. Herrick MK. Pathology of pineal tumors. In: Neuwelt EA, ed. *Diagnosis and treatment of pineal region tumors*. Baltimore: Williams & Wilkins, **1984**:31–60
27. Sano K. Pineal region tumors: problems in pathology and treatment. *Clin Neurosurg* **1983**;30:59–91
28. Ueki K, Tanaka R. Treatments and prognosis of pineal tumours—experience of 110 cases. *Neurol Med Chir* (Tokyo) **1980**;20:1–26
29. Shinoda J, Yamada H, Norboru S, Ando, Takashi, Hirata T, Miwa Y. Placental alkaline phosphatase as a tumor marker for primary intracranial germinoma. *J Neurosurg* **1988**;68:710–720
30. Shinoda J, Miwa Y, Sakai N, et al. Immunohistochemical study of placental alkaline phosphatase in primary intracranial germ-cell tumors. *J Neurosurg* **1985**;63:733–739
31. Vorkapic P, Waldhauser F, Bruckner R, Biegelmayer C, Schmidbauer M, Pendl G. Serum melatonin levels: a new neurodiagnostic tool in pineal region tumors? *Neurosurgery* **1987**;21:817–824
32. Phillips PC, Kremzner LT, De Vivo DC. Cerebrospinal fluid polyamines: biochemical markers of malignant childhood brain tumors. *Ann Neurol* **1986**;19:360–364